Star Formation Newsletter No. 332, #69-75

69. Possible Time Correlation Between Jet Ejection and Mass Accretion for RW Aur A, Takami et al., ApJ, 901, 24
70. The Excitation Conditions of CN in TW Hya, Teague & Loomis, ApJ, 899, 157
71. A wide survey for circumstellar disks in the Lupus complex, Teixeira et al., A&Ap, P. S Teixeira et al., A&Ap,
72. Giant planet formation models with a self-consistent treatment of the heavy elements, Valletta & Helled, ApJ, 990, 133
73. Measurements of the Ca II infrared triplet emission lines of pre-main-sequence stars, Yamashita et al., PASJ, 73,
74. Cloud-cloud collision as drivers of the chemical complexity in Galactic Centre molecular clouds, Zeng et al., MNRAS, 497, 4896
75. Fragmentation of star-forming filaments in the X-shape Nebula of the California molecular cloud, Zhang et al., A&Ap, 642, A76

花輪 知幸 (千葉大)

No. 69. Possible Time Correlation Between Jet Ejection and Mass Accretion for RW Aur A, Takami et al., ApJ, 901, 24

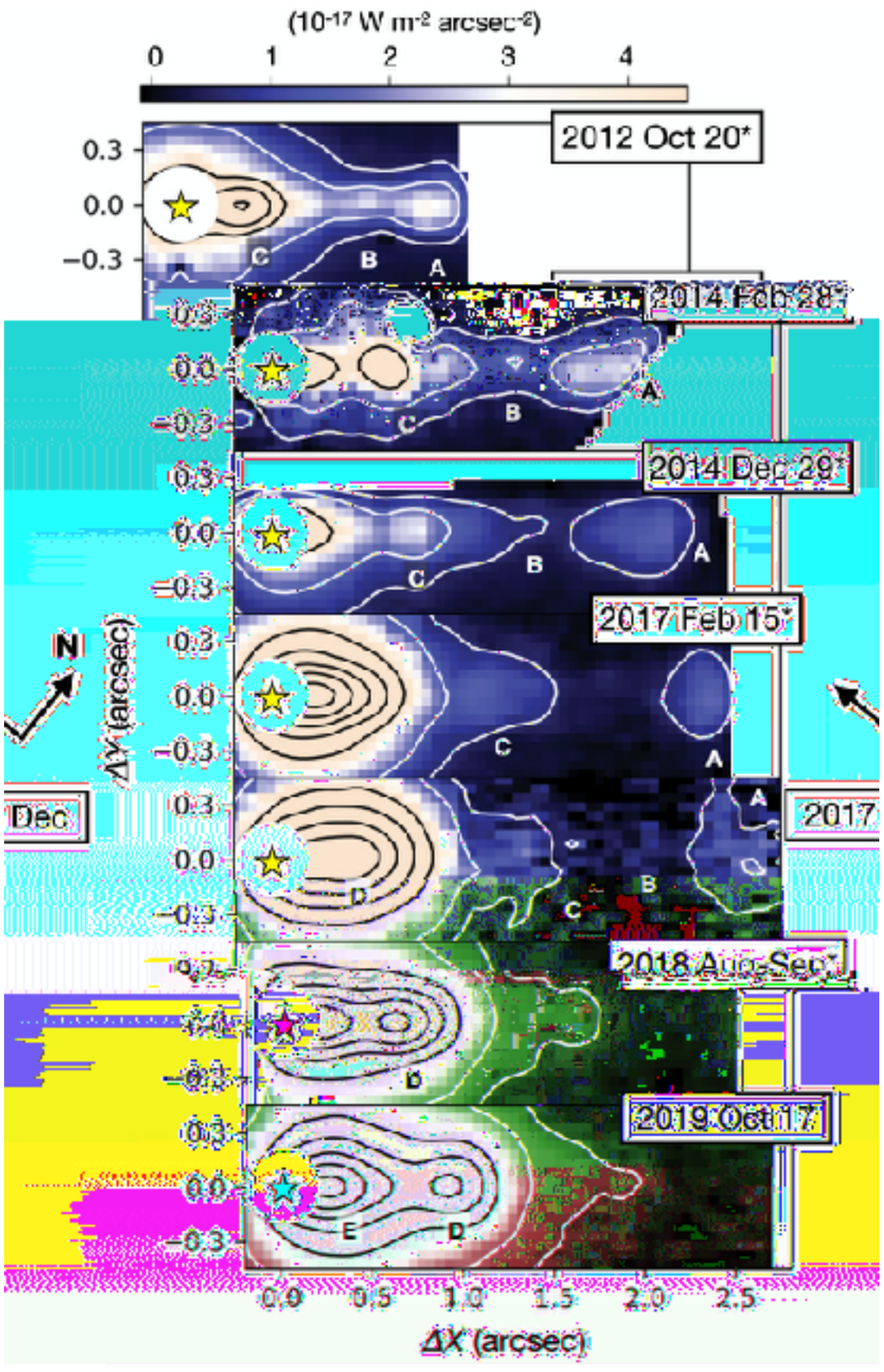

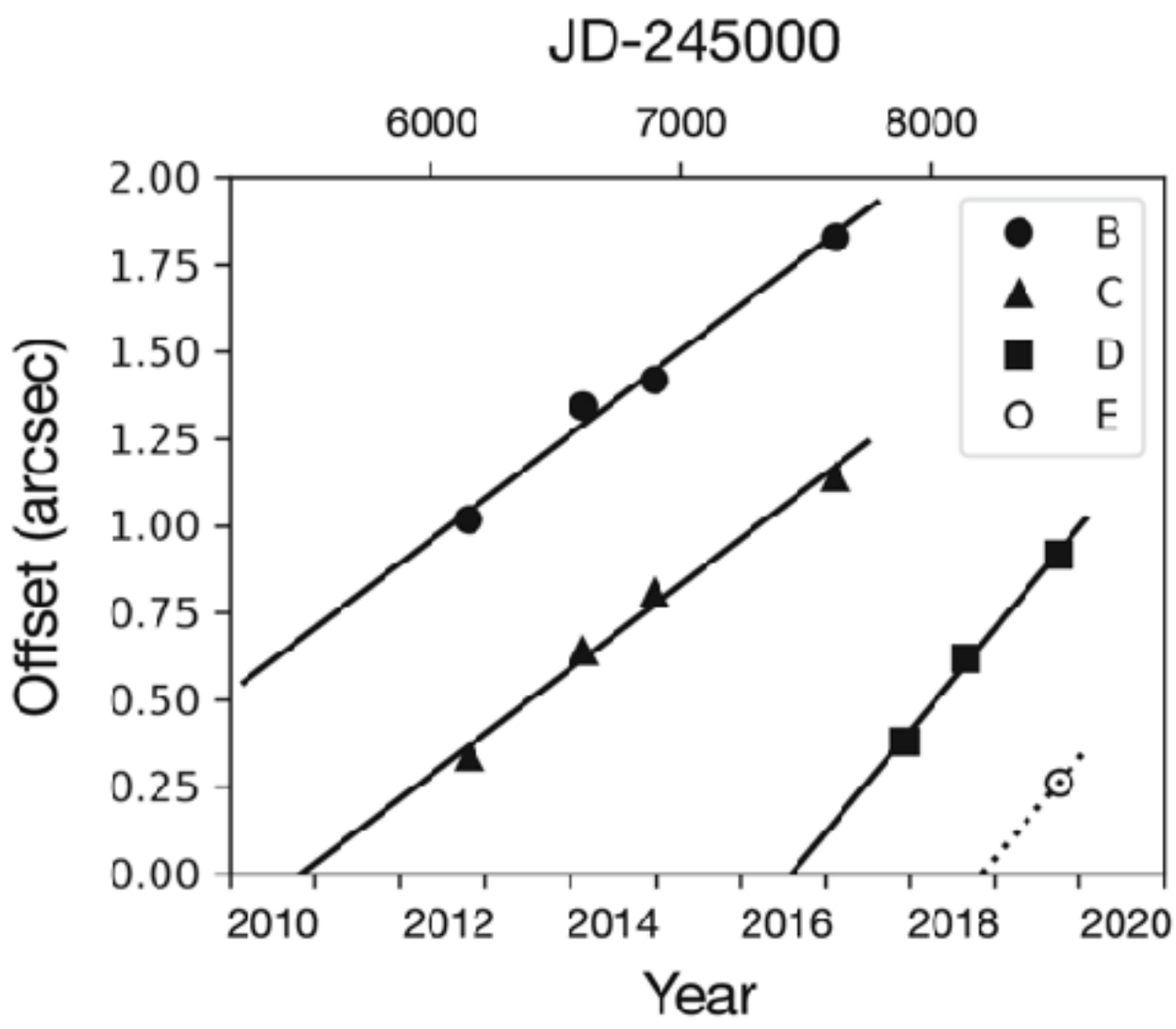

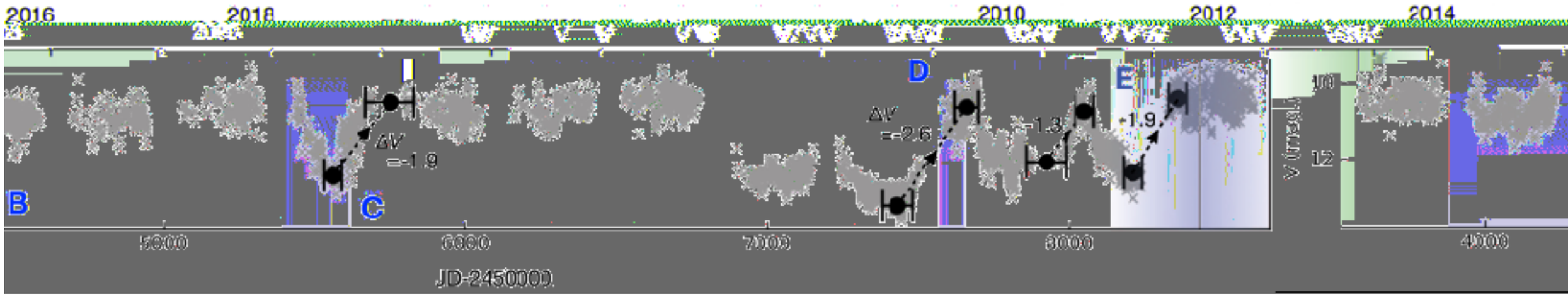
2016
2018
2010
2012
2014
B
C
D
E
ΔV =-1.9
ΔV =-2.6
-1.3
-1.9
JD-2450000

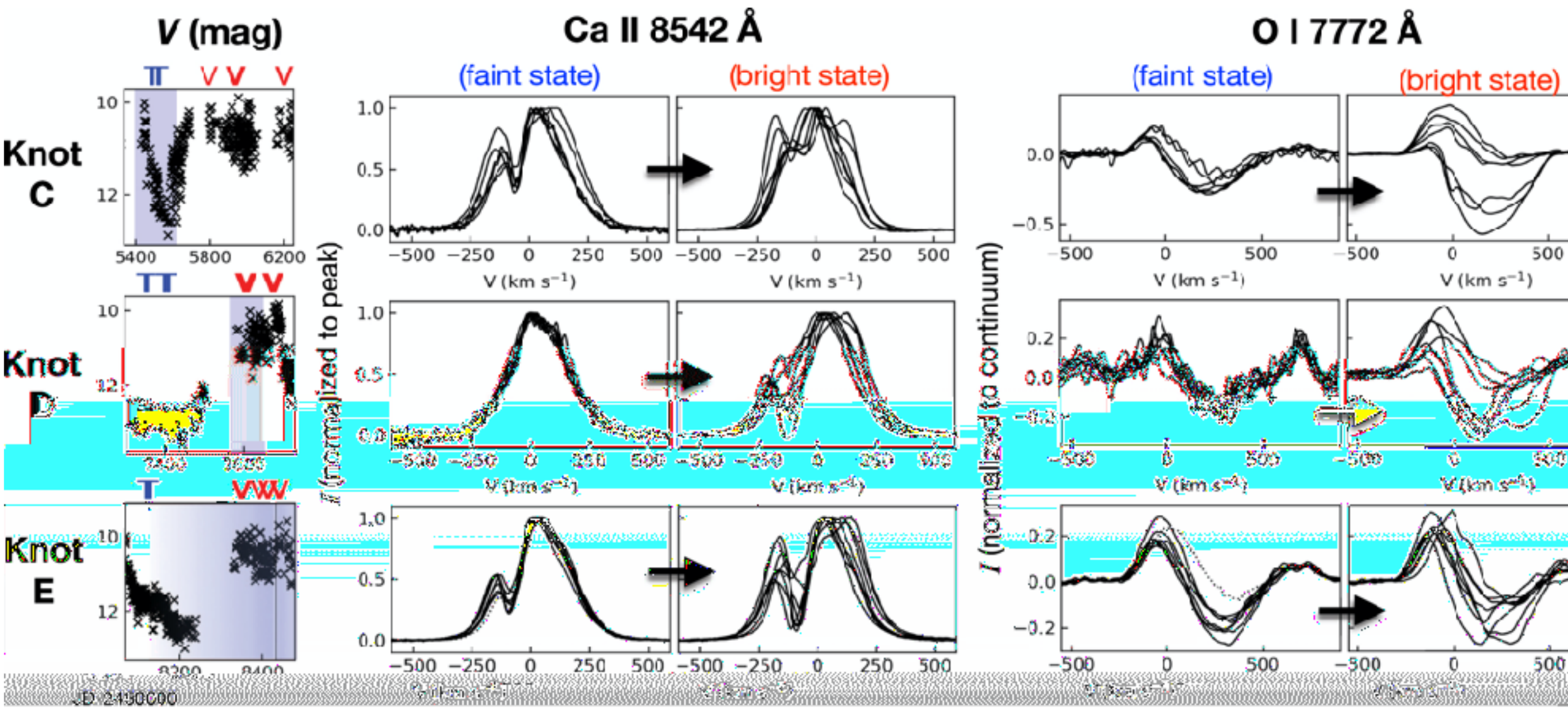
V (mag)
Ca II 8542 Å
O I 7772 Å
(faint state)
(bright state)
Knot C
Knot D
Knot E
I (normalized to peak)
I (normalized to continuum)
V (km s^{-1})
JD-2450000

No. 70. The Excitation Conditions of CN in TW Hya, Teague & Loomis, ApJ, 899, 157

24 hyperfine transitions

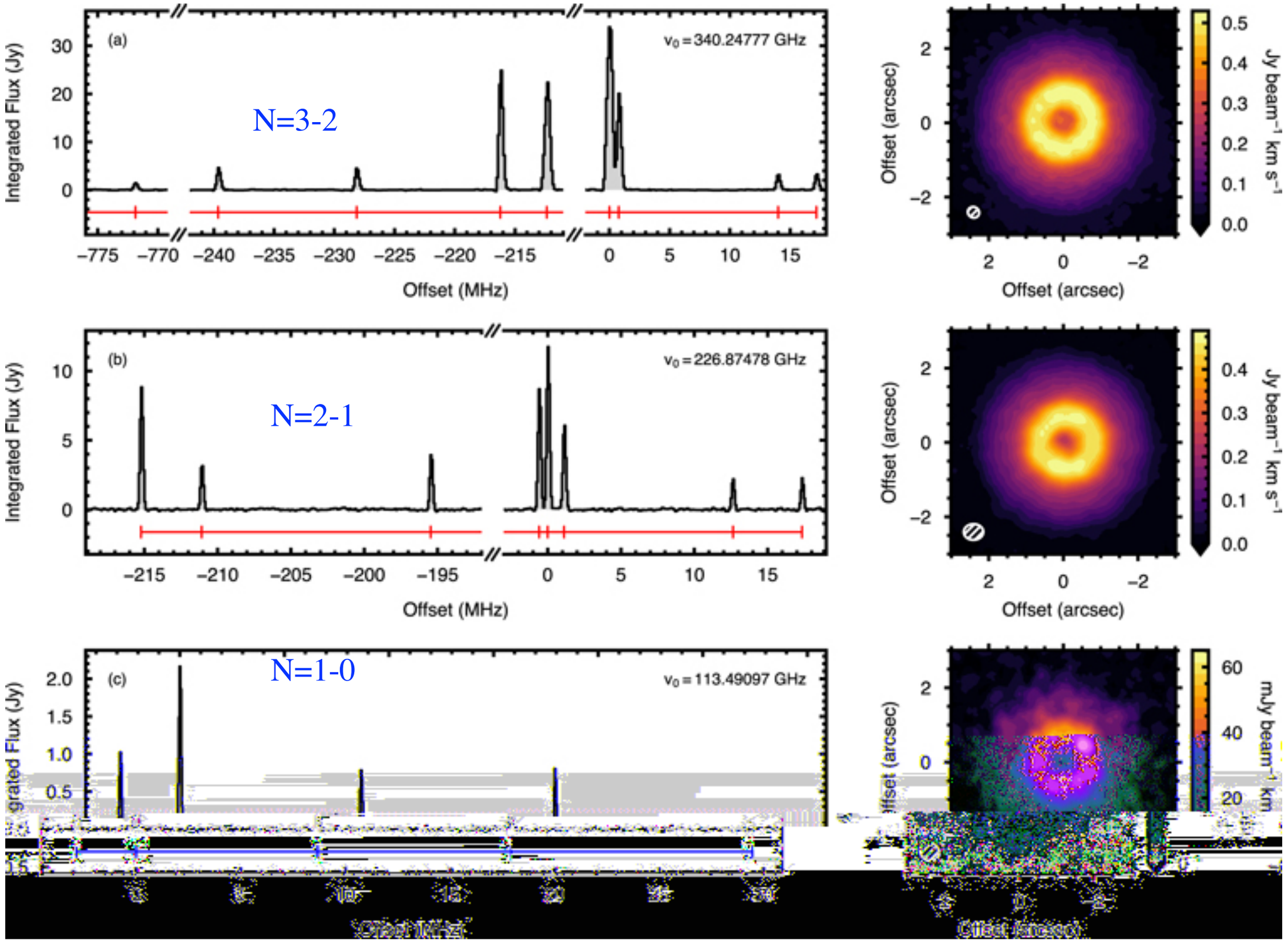

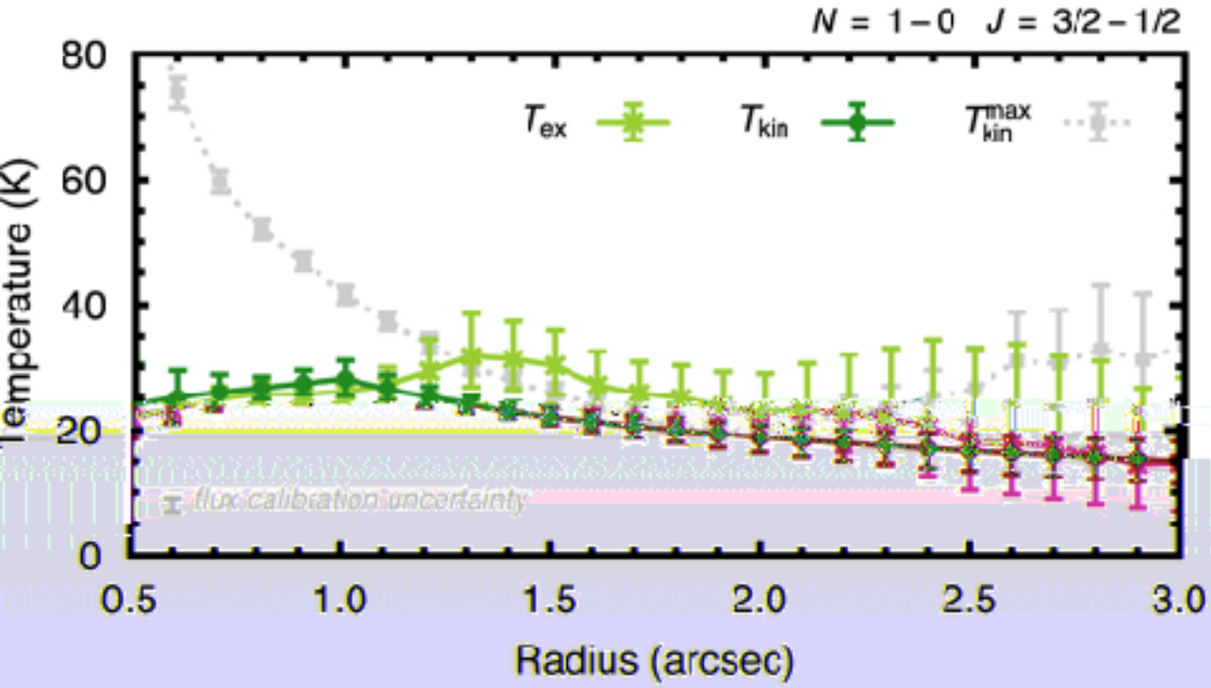
N = 1 – 0 J = 3/2 – 1/2
T_ex
T_kin
T_kin^max
flux calibration uncertainty
Temperature (K)
Radius (arcsec)

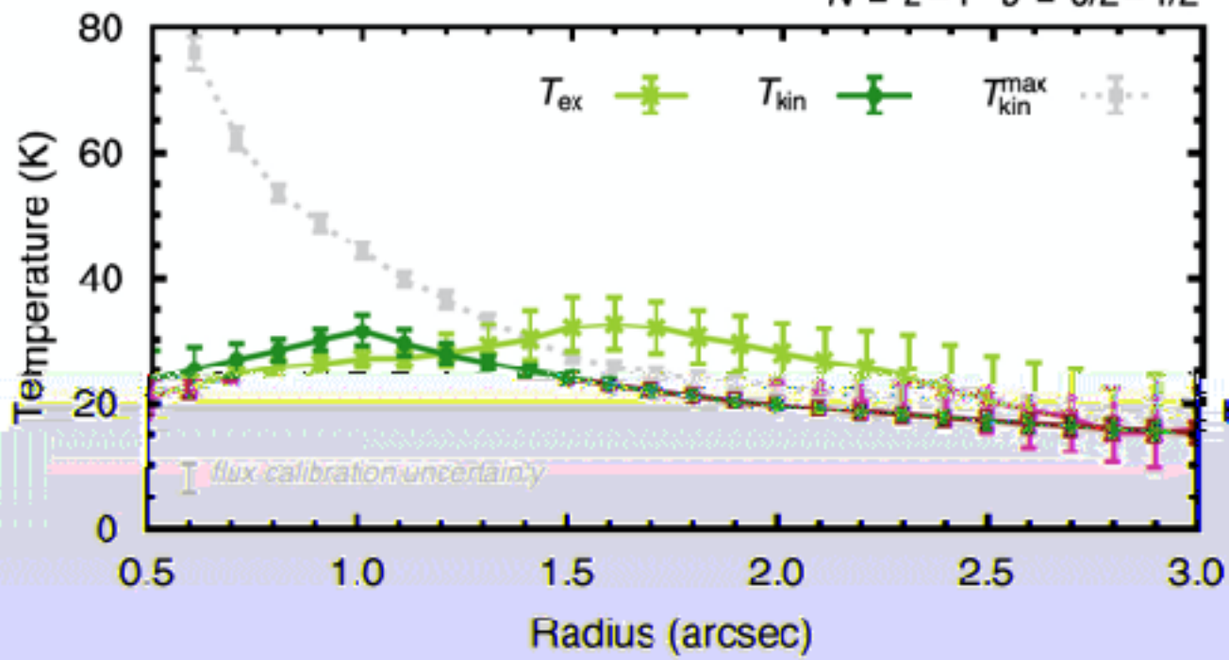
N = 2 – 1 J = 3/2 – 1/2
T_ex
T_kin
T_kin^max
flux calibration uncertainty
Temperature (K)
Radius (arcsec)

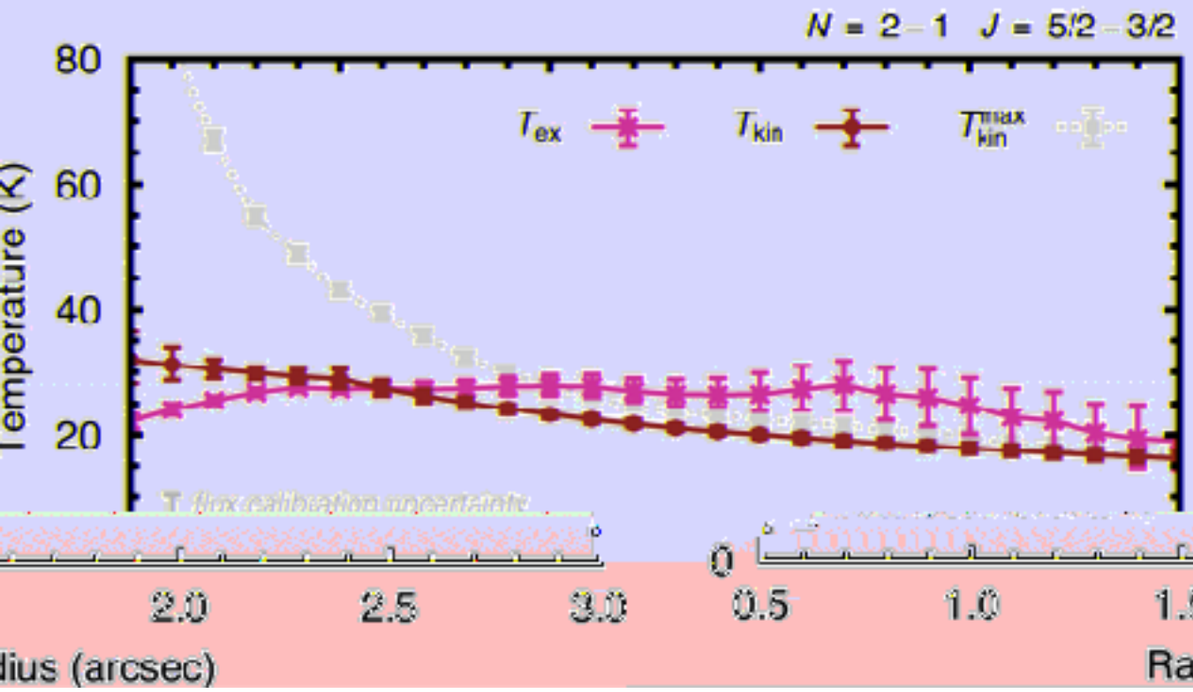
N = 2 – 1 J = 5/2 – 3/2
T_ex
T_kin
T_kin^max
flux calibration uncertainty
Temperature (K)
Radius (arcsec)

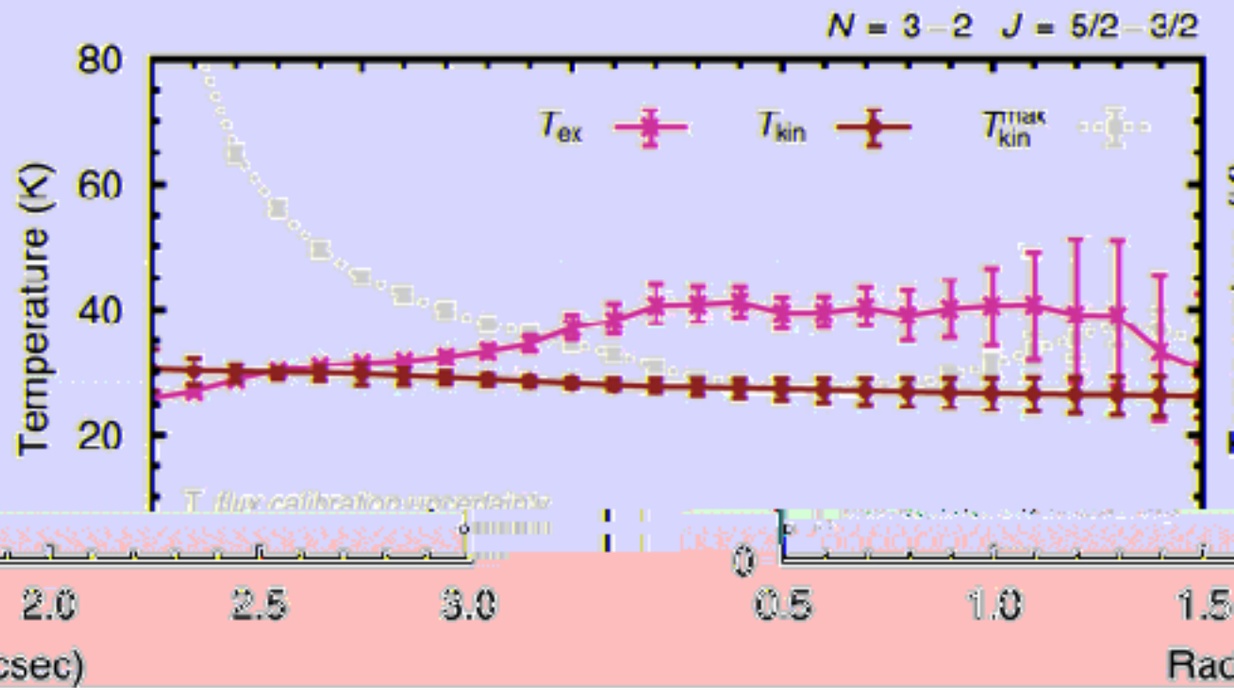
N = 3 – 2 J = 5/2 – 3/2
T_ex
T_kin
T_kin^max
flux calibration uncertainty
Temperature (K)
Radius (arcsec)

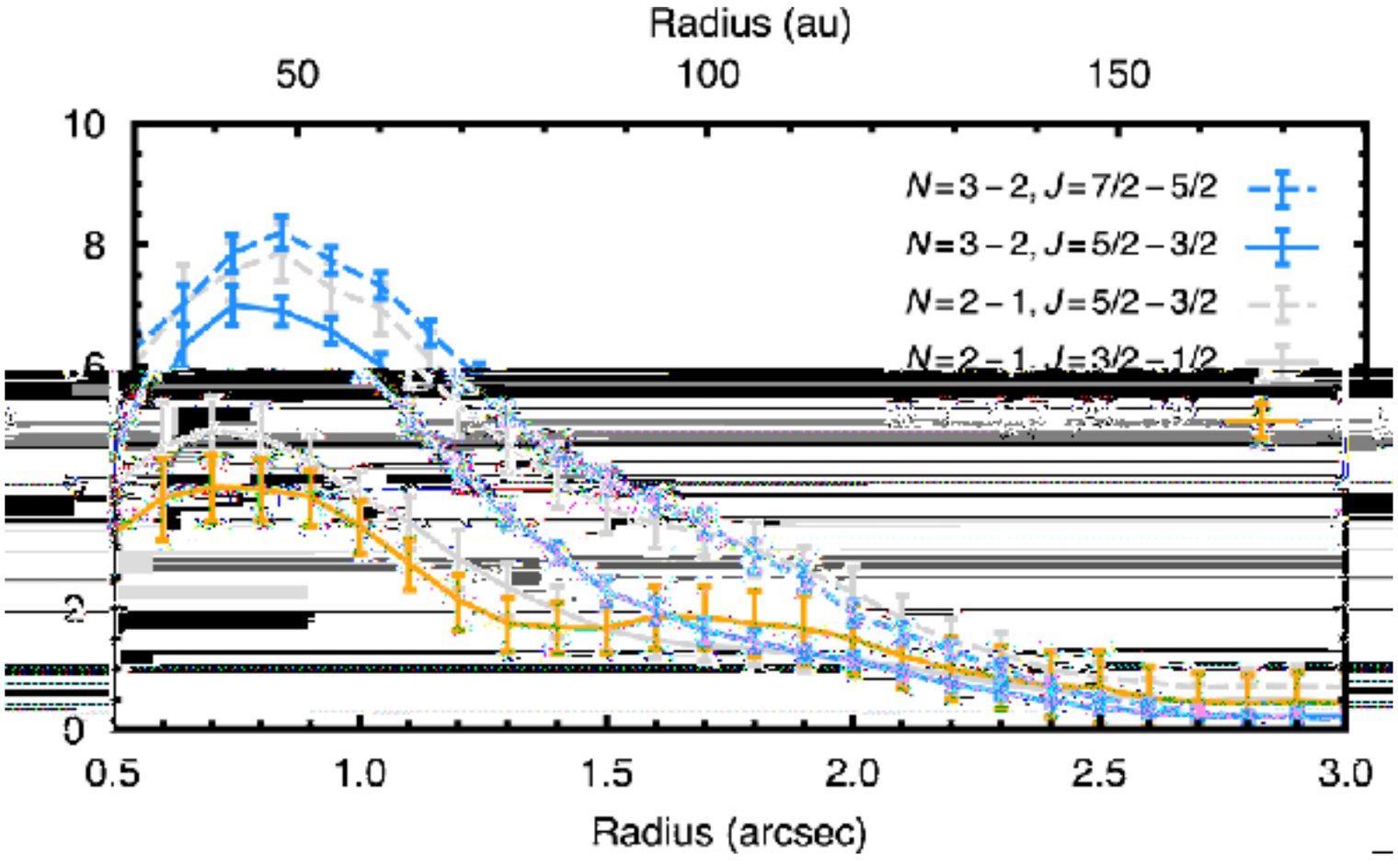

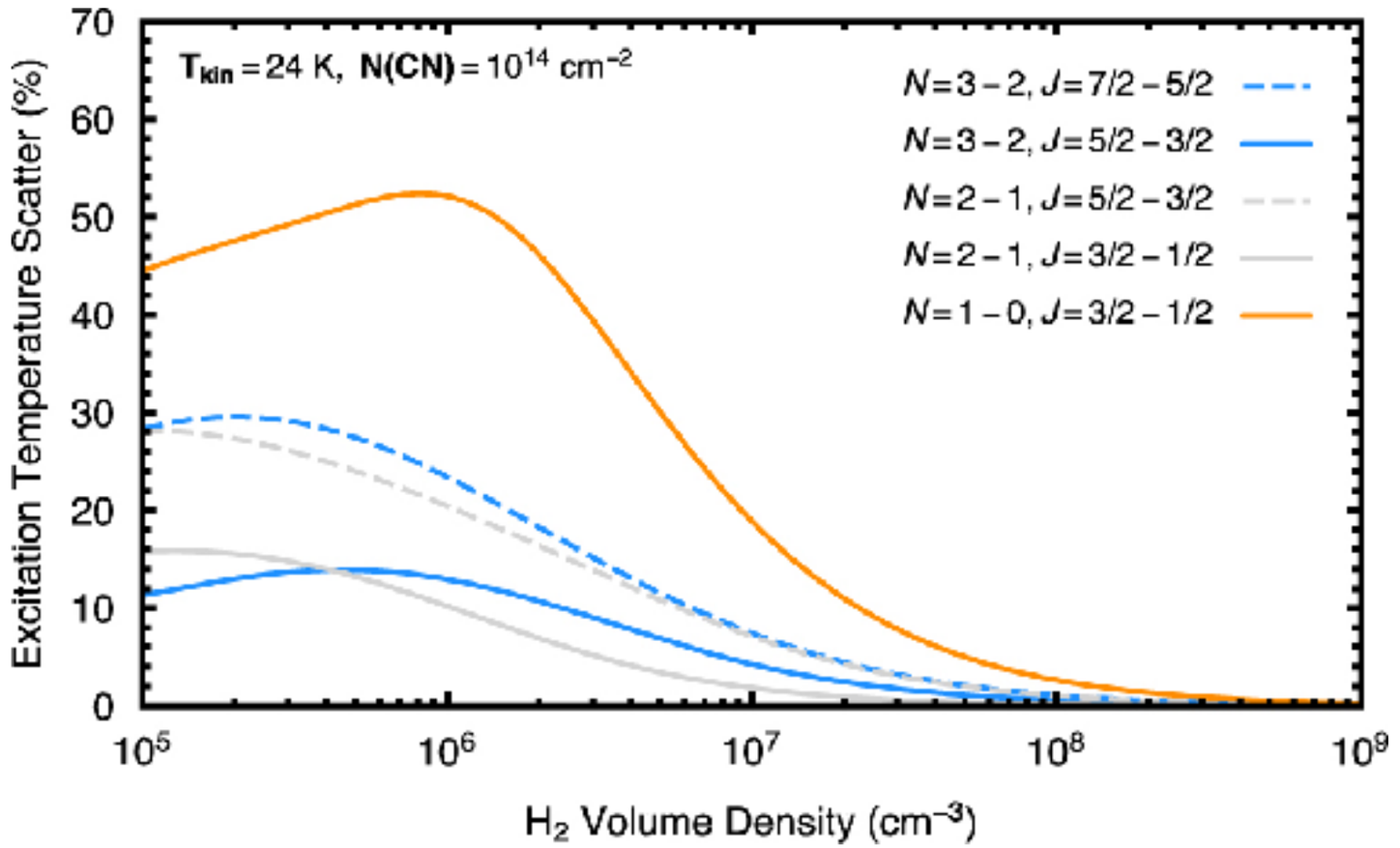

LTE では合わない

著者の年来の主張

対立グループがいる

No. 71. A wide survey for circumstellar disks in the Lupus complex, Teixeira et al., A&Ap, P. S Teixeira et al., A&Ap, 642, A86

Gaia DR2 + WISE **の** color data **をもとに** 494**平方度の領域で円盤をもつ星を同定。**56 new sources with thick disk 42 new sources with anemic disk.

これらの領域は繋がっている。

YSO age < 4 Myr　　4 Myr < YSO age < 12 Myr　　12 Myr < YSO age

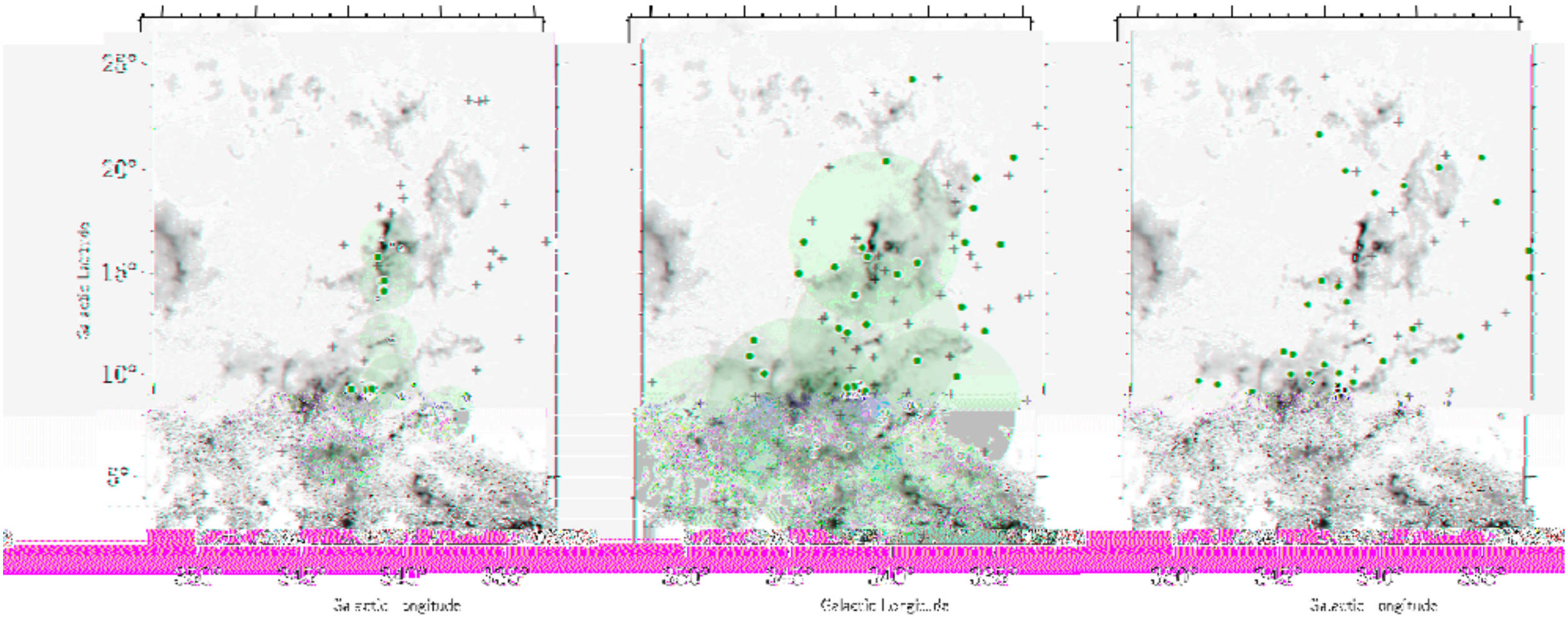

$\lambda = 3.6, 4.6, 11.6\ \mu m$

No. 72. Giant Planet Formation Models with a Self-consistent Treatment of the Heavy Elements, Valletta & Helled, ApJ, 900, 133

MESA　(1**次元，恒星進化) を拡張**

降着ガスに H_2O **の** pebble **が混じる効果を取り込む**

Opacity, **状態方程式(潜熱)の変化を取り入れる**

重い元素は $\alpha_{mlt} = 0.1$ **の**Mixing length theory **で計算**

Table 1
The Various Heavy-element Accretion Rates used in This Work

Heavy-element Accretion rate	Reference	Size	Density	Disk's Viscosity
$\dot{M}_Z1$	Pollack et al. (1996), their Equation (1)	100 km	$\sigma = 10$ g cm^{-2}	...
$\dot{M}_Z2$	Lambrechts & Johansen (2014), their Equation (31)	~1 cm	$\Sigma = 50$ g cm^{-3}	$\alpha = 10^{-3}$
$\dot{M}_Z3$	Lambrechts & Johansen (2014), their Equation (31)	~1 cm	$\Sigma = 50$ g cm^{-3}	$\alpha = 10^{-5}$
$\dot{M}_Z4$	Fortier et al. (2007), their Equation (10)	100 km	$\sigma = 10$ g cm^{-2}	...
$\dot{M}_Z5$	Shiraishi & Ida (2008), their Equation (24) and 25	100 km	$\sigma = 10$ g cm^{-2}	...

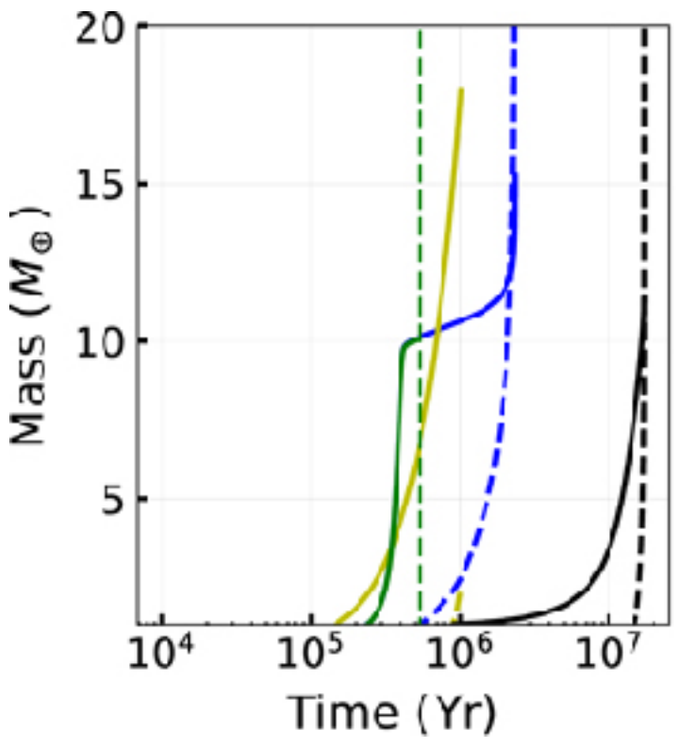

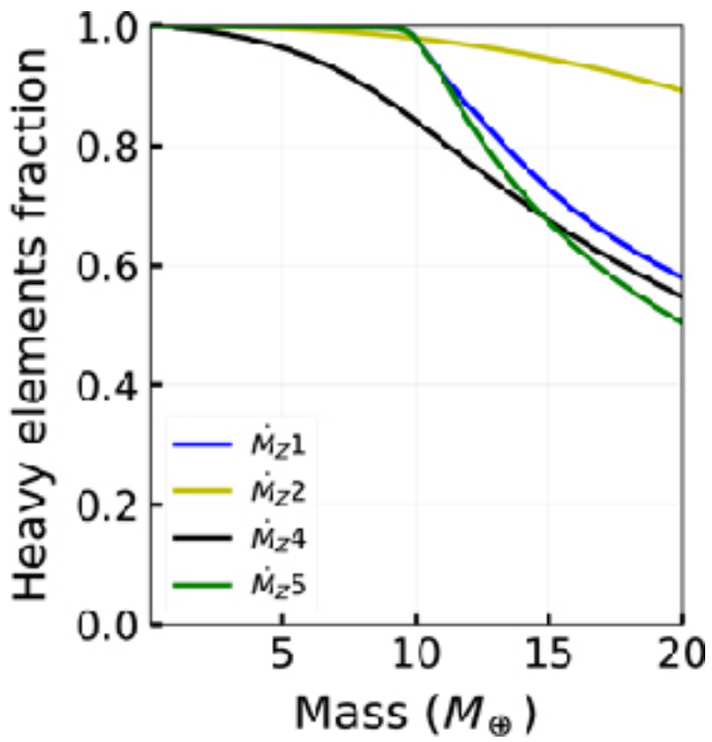

Heavy element **により惑星形成の時間が短くなる(ただし既知の結果)**

No. 73. Measurements of the Ca II infrared triplet emission lines of pre-main-sequence stars, Yamashita et al., PASJ, 72, 80

Ca II infrared triplet lines (λλ8498, 8542, 8662 Å) of 60 PMS stars.

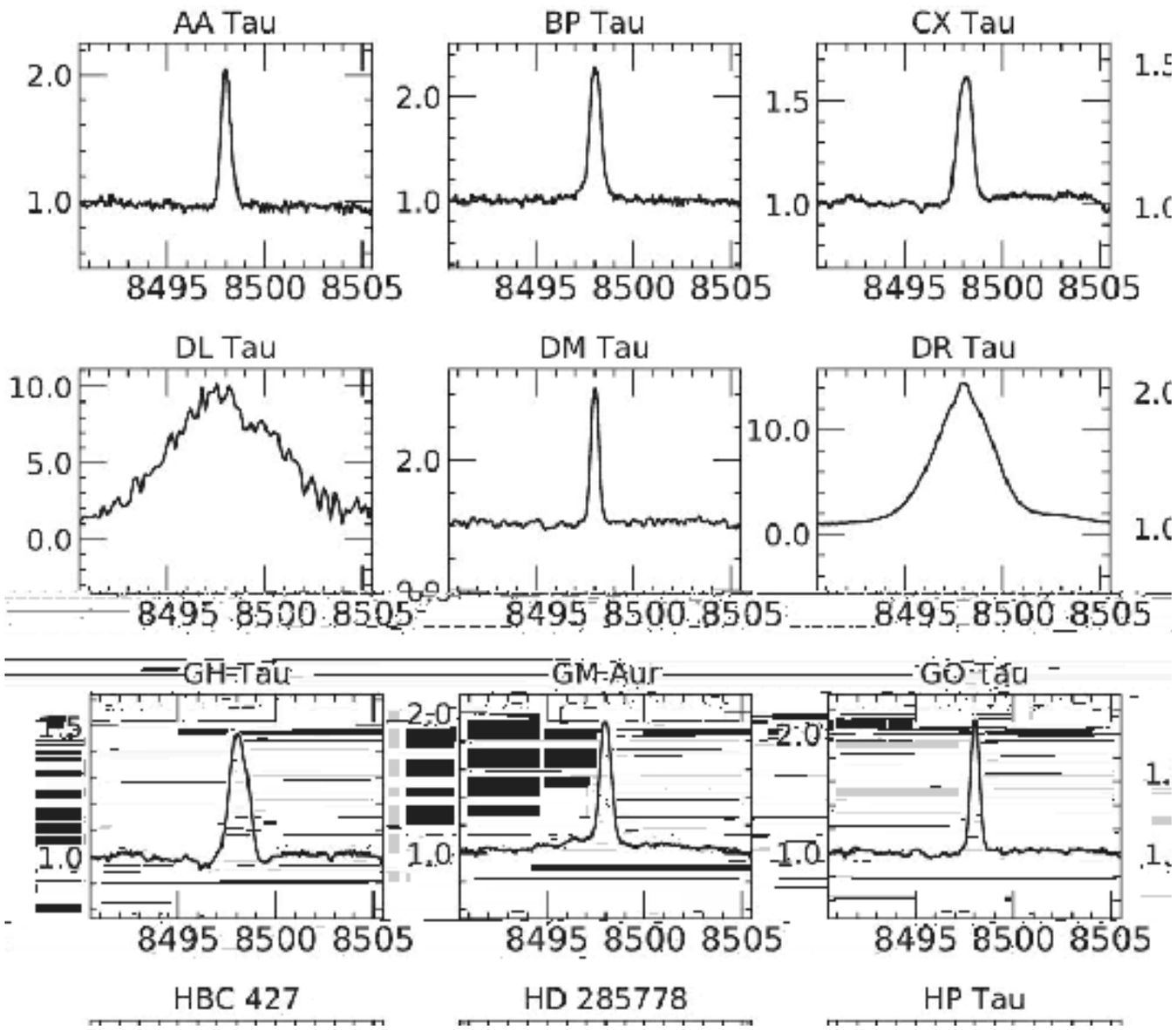

$W_{\lambda 8542}/W_{\lambda 8498}$ = 1.0–2.0, $W_{\lambda 8662}/W_{\lambda 8498}$ = 0.7–1.7 **は** PMS stars **と** young open cluster **中の低質量星で共通。**

DG Tau, DL Tau, DR Tau, RY Tau, SU Aur, RECX 15, RXJ1147.7–7842 **は広い輝線**

赤外輝線はChrmospheric activity **による ものではないか**

No. 74. Cloud-cloud collision as drivers of the chemical complexity in Galactic Centre molecular clouds, Zeng et al., MNRAS, 497, 4896

G+0.693-0.03はなぜCOMが豊富?

SMA, APEX

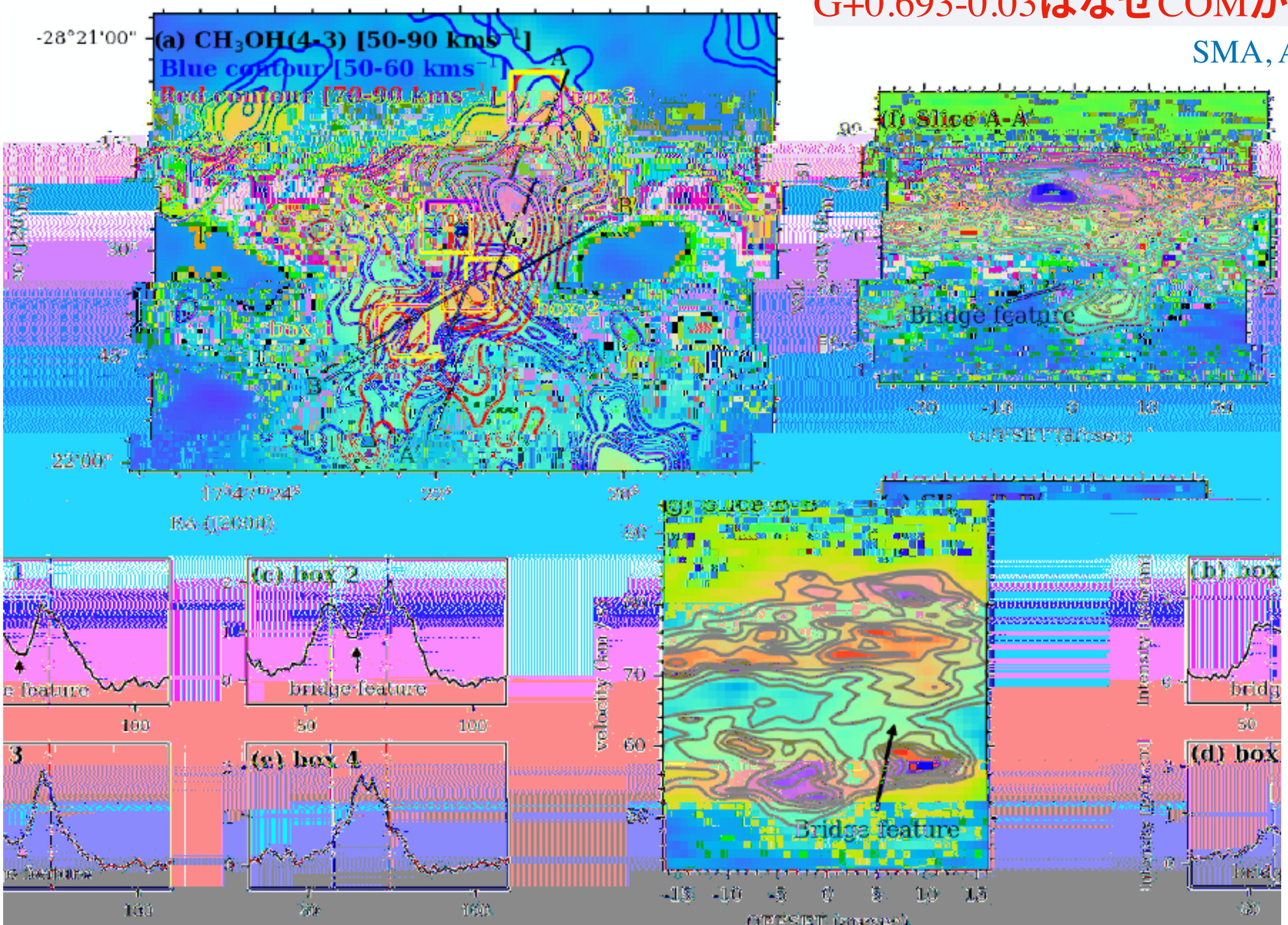

連続波は強くない

class I methanol maser

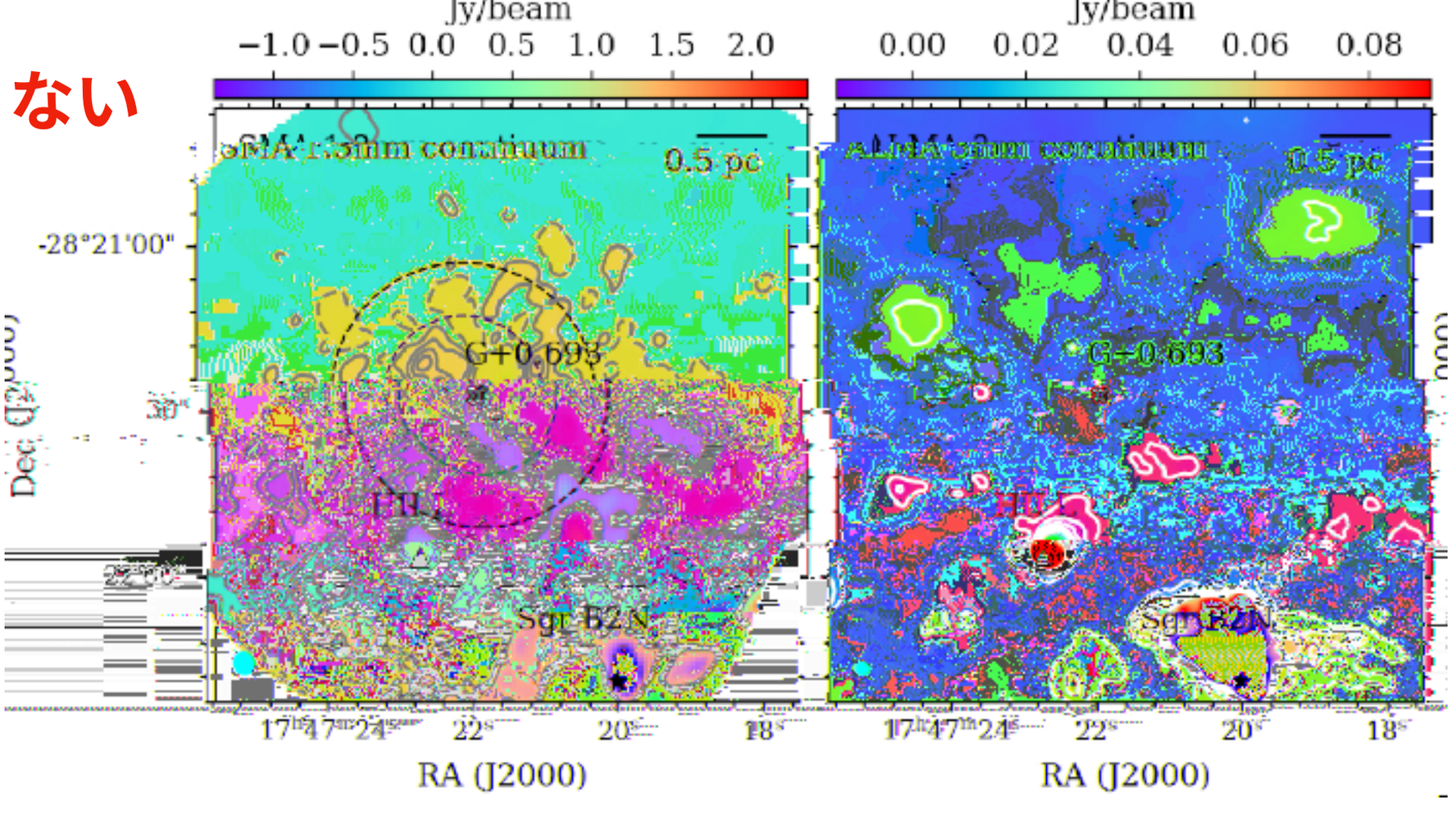

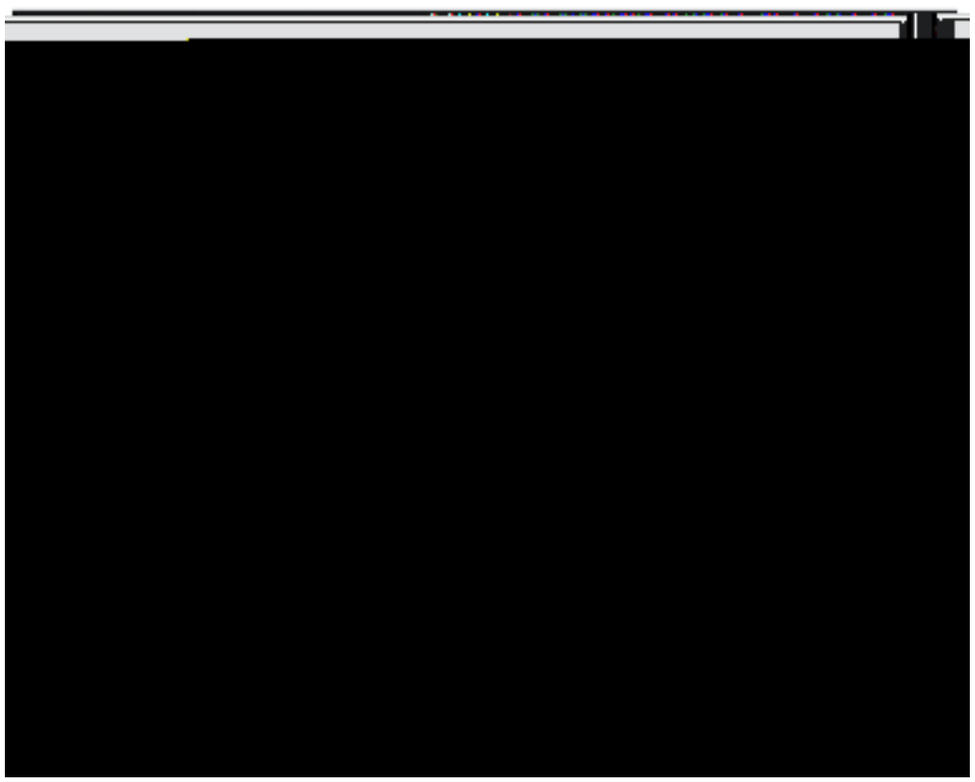

+ G+0.693
● Sgr B2N
● Sgr B2M

No. 74. Fragmentation of star-forming filaments in the X-shape Nebula of the California molecular cloud, Zhang et al., A&Ap, 642, A76

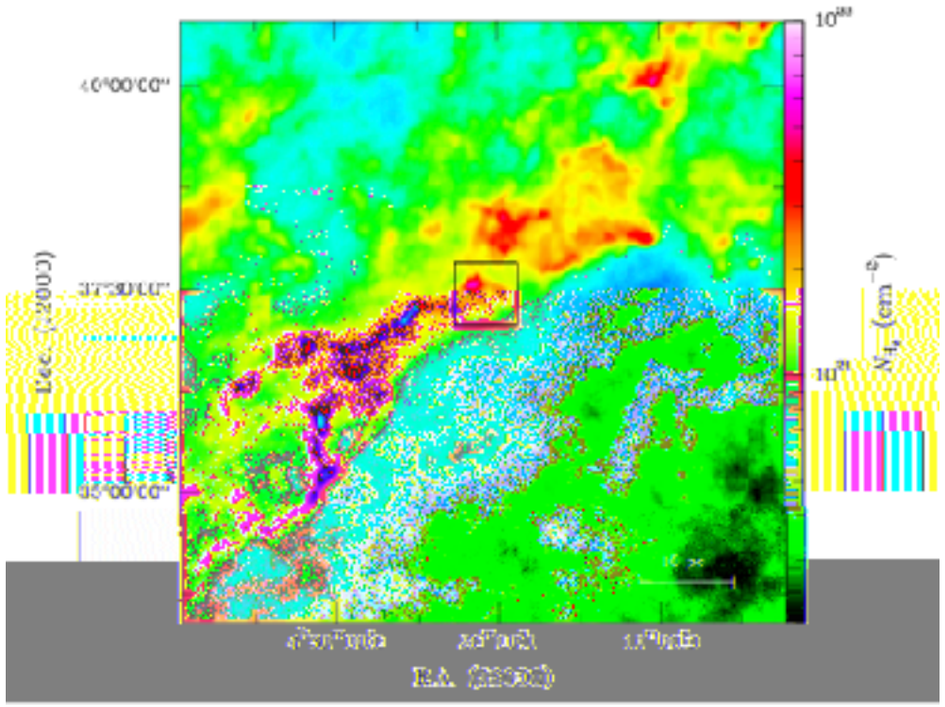

Planck 850 μm optical-depth data (5′ resolution).

Herschel

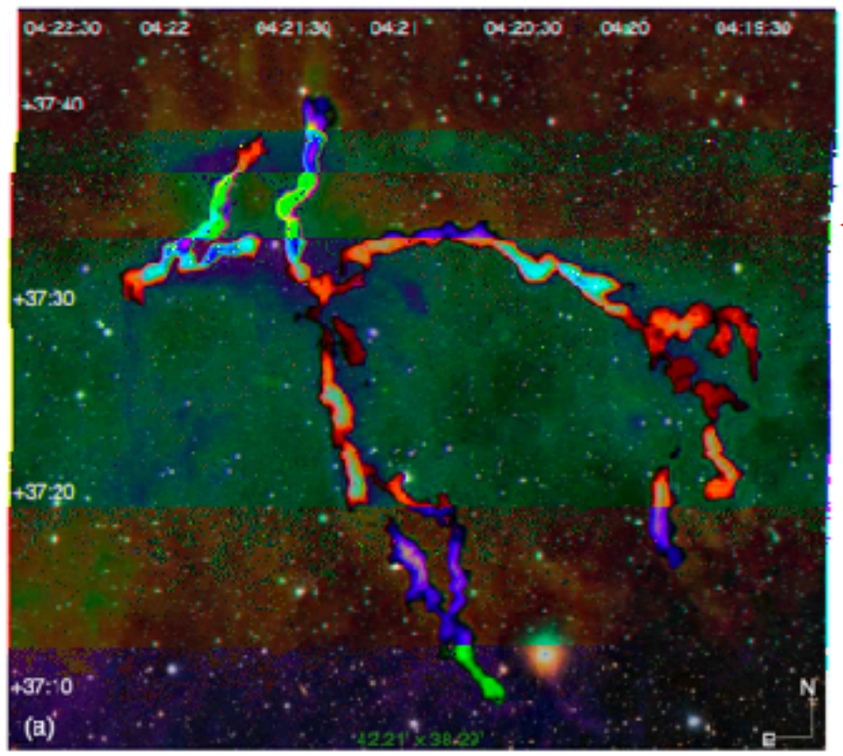

フィルタ
リング

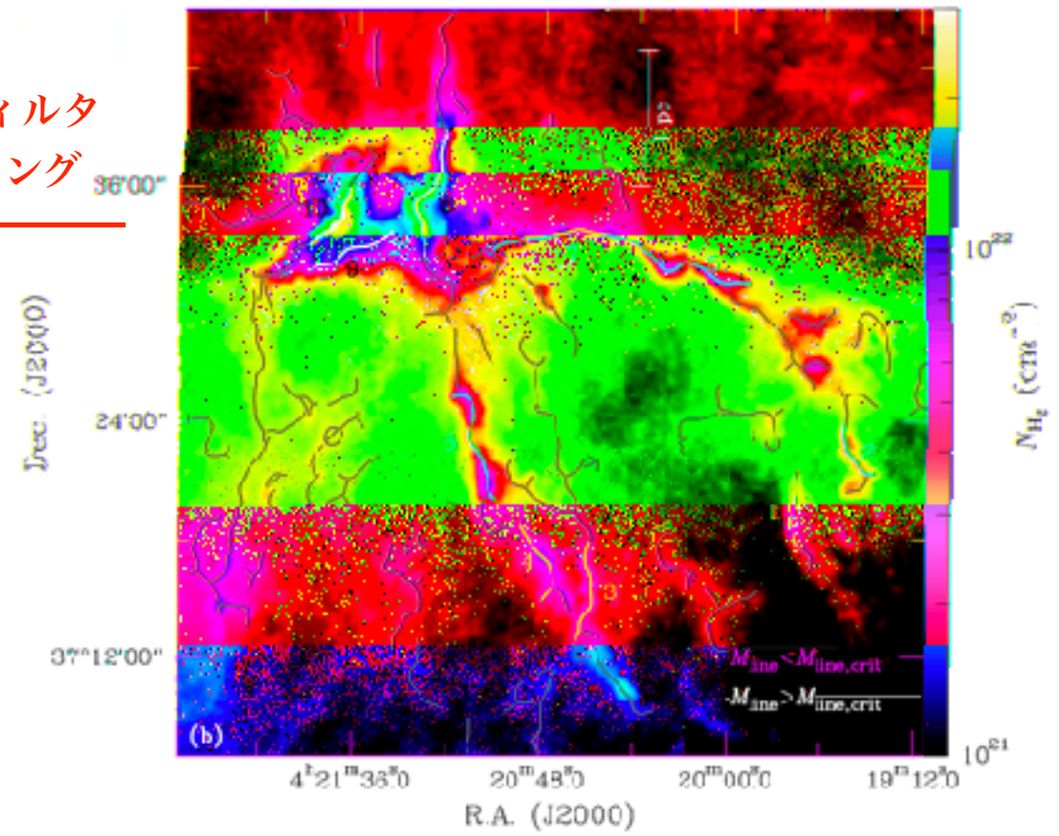

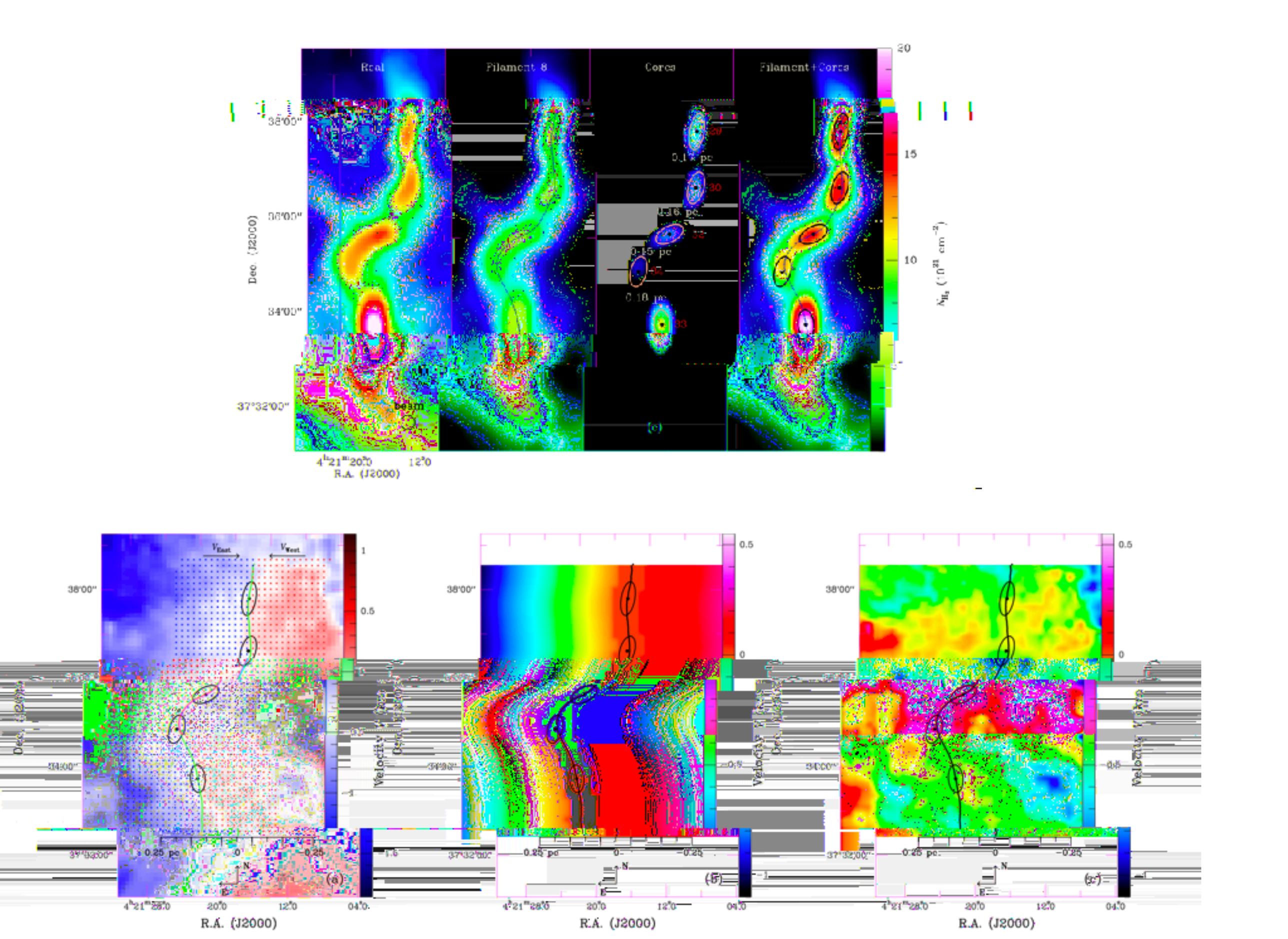
Real
Filament 8
Cores
Filament+Cores
38'00"
36'00"
34'00"
Dec. (J2000)
37°32'00"
0.14 pc
0.16 pc
0.15 pc
0.18 pc
20
30
35
45
33
(c)
20
15
10
5
N_{H_2} ($\times 10^{21}$ cm^{-2})
4^{h}21^{m}20^s.0
12^s.0
R.A. (J2000)
V_{East}
V_{West}
1
0.5
0.25 pc
0
−0.25
N
E
(a)
0.5
0
Velocity
1.6
−0.5
(b)
(d)